Superconductivity from undressing. II. Single-particle Green's function and photoemission in cuprates

J. E. Hirsch
Department of Physics, University of California, San Diego, La Jolla, California 92093-0319
(Received 24 July 2000)

Experimental evidence indicates that the superconducting transition in high-T_c cuprates is an ''undressing'' transition. Microscopic mechanisms giving rise to this physics were discussed in the first paper of this series. Here we discuss the calculation of the single-particle Green's function and spectral function for Hamiltonians describing undressing transitions in the normal and superconducting states. A single parameter Υ describes the strength of the undressing process, and drives the transition to superconductivity. In the normal state, the spectral function evolves from predominantly incoherent to partly coherent as the hole concentration increases. In the superconducting state, the ''normal'' Green's function acquires a contribution from the anomalous Green's function when Υ is nonzero; the resulting contribution to the spectral function is *positive* for hole extraction, and *negative* for hole injection. It is proposed that these results explain the observation of sharp quasiparticle states in the superconducting state of cuprates along the $(\pi,0)$ direction, and their absence along the (π,π) direction.

I. INTRODUCTION

Photoemission and optical experiments indicate that in high-T_c cuprates a transition from an incoherent state to a partially coherent state occurs both as the hole doping increases in the normal state and as the system becomes superconducting.[1–4] Basov *et al.*[4] observed a lowering of *c*-axis kinetic energy as the transition to the superconducting state occurs in several cuprates, especially in the underdoped situation. It was established, however, that the *magnitude* of the *c*-axis kinetic-energy lowering detected is far too small to account for the superconducting condensation energy at least in some cuprates.[5] Ding *et al.*,[1] Campuzano and coworkers,[6,7] and Feng *et al.*[2] reported observations of sharp quasiparticle peaks in the superconducting state in angle-resolved photoemission emerging from a highly incoherent normal-state background along the $(\pi,0)$ direction, close to the $(\pi/a,0)$ point. Ding *et al.* interpreted the photoemission peak in terms of an enhanced quasiparticle weight Z in the superconducting state, and Feng *et al.*[2] suggested that the peak in photoemission is a signature of the superfluid density. Norman *et al.*[7] analyzed the photoemission observations in terms of a ''mode model,'' and emphasized the close connection between their observations and Basov *et al.*'s observation of kinetic-energy lowering. Furthermore, Basov *et al.* emphasized that kinetic-energy lowering seems to occur only when there is a high degree of incoherence in the normal state, and appears to vanish as the normal state becomes more coherent (overdoped regime).[4] They furthermore proposed that the photoemission experiments suggest that kinetic-energy lowering may also occur *in plane* in the cuprates albeit only along the $(\pi,0)$ direction, and for this reason may be difficult to observe directly.

The model of hole superconductivity[8,9] *predicted*, before the experimental observations, that the superconducting condensation energy originates in in-plane kinetic energy lowering[10] and arises from a process of *undressing of hole carriers* as the pairing state develops.[11] Thus it describes both the kinetic-energy lowering, arising from the low-energy effective Hamiltonian, as well as the high-energy optical spectral weight transfer, that was also observed experimentally.[12] In the first paper of this series[13] (hereafter referred to as I) we formulated more generally the principles of superconductivity through hole undressing, and pointed out that this physics would show up both in the one- and two-particle Green's functions, in qualitative agreement with the observations reported above. Here we report a calculation of the single-particle Green's function and spectral weight in the superconducting state, and discuss the implications for the understanding of photoemission experiments.

II. GENERAL PRINCIPLES

In the class of models discussed in I, the wave-function renormalization of quasiparticles is a function of the site occupation in a local representation. The wave-function renormalization arises from coupling to a local boson degree of freedom. Three examples of specific microscopic Hamiltonians describing this physics were discussed in I. The ''coherent'' part of the electron creation operator at site i is defined by the transformation

$$d^\dagger_{i\sigma}=[T-(T-S)\tilde{n}_{di,-\sigma}]\tilde{d}^\dagger_{i\sigma}, \tag{1}$$

with $0\leqslant S<T\leqslant 1$. The $\tilde{d}$ operators in Eq. (1) are quasiparticle operators,[14] and $\tilde{n}_d$ is the electron site occupation. Equation (1) expresses the fact that the electron becomes less coherent as more electrons are added to the band. It should be kept in mind that the coherent part of the electron operator on the left side of Eq. (1) is not the full electron creation operator, as it does not contain terms that give rise to excited states of the boson degree of freedom.[13]

It will be more useful to use hole operators rather than electron operators throughout this paper; we stress, however, that the discussion can be consistently carried out in electron

as well as hole representations. In terms of hole operators, the coherent part of the hole creation operator is

$$c_{i\sigma}^{\dagger}=[S+(T-S)\tilde{n}_{i,-\sigma}]\tilde{c}_{i\sigma}^{\dagger}\equiv S[1+\Upsilon\tilde{n}_{i,-\sigma}]\tilde{c}_{i\sigma}^{\dagger}. \quad (2)$$

Equation (2) expresses the fact that the hole quasiparticle weight will increase with the local hole concentration, from S in the regime of low hole concentration to T for high hole concentration. The high degree of incoherence observed in high-T_c cuprates for low hole doping implies $S\ll 1$, and the fact that coherence is achieved for relatively small values of hole doping implies that the ''undressing parameter''

$$\Upsilon=\frac{T}{S}-1 \quad (3)$$

is very large. Υ is the parameter that drives the transition to a superconducting state. Note that a large Υ necessarily implies $S\ll 1$, due to the constraint $T\leqslant 1$. For the normal state, Eq. (2) implies, for the hole operator,

$$c_{i\sigma}^{\dagger}=S\left[1+\frac{n}{2}\Upsilon\right]\tilde{c}_{i\sigma}^{\dagger}, \quad (4)$$

with n the hole concentration per site, and

$$n_{i\sigma}=S^2\left[1+\frac{n}{2}\Upsilon\right]^2\tilde{n}_{i\sigma}\equiv Z(n)\tilde{n}_{i\sigma} \quad (5)$$

for the hole number operator, with $Z(n)$ the hole quasiparticle weight. Equation (5) implies that hole quasiparticles in the normal state become more coherent as the hole concentration increases. In the limit $S\rightarrow 0$, quasiparticles become completely incoherent in the normal state for low hole concentration, and Fermi-liquid theory breaks down. This limit is also described by the theory; in this limit, the transition to the superconducting state is a superconductor-insulator transition.[15,16] Even though for that particular limiting situation Fermi-liquid theory does not describe the normal state, we stress that our approach is *not* a ''non-Fermi-liquid'' approach, but instead is deeply rooted in Fermi-liquid theory.

Consider the bare kinetic energy in a tight-binding model in terms of hole operators:

$$H_{kin}=-\sum_{i,j,\sigma}t_{ij}^{0}(c_{i\sigma}^{\dagger}c_{j\sigma}+\text{H.c.}). \quad (6)$$

Replacement of the bare hole operators by the quasiparticle operators, using Eq. (2), yields

$$H_{kin}=-\sum_{i,j,\sigma}t_{ij}^{\sigma}(\tilde{c}_{i\sigma}^{\dagger}\tilde{c}_{j\sigma}+\text{H.c.}) \quad (7a)$$

$$t_{ij}^{\sigma}=t_{ij}^{0}S^2[1+\Upsilon(\tilde{n}_{i,-\sigma}+\tilde{n}_{j,-\sigma})+\Upsilon^2\tilde{n}_{i,-\sigma}\tilde{n}_{j,-\sigma}]. \quad (7b)$$

Equation (7) expresses the fact that the hopping amplitude of a hole quasiparticle will be increased, and as a consequence its kinetic energy will be lowered, as the local hole concentration increases; this is a direct consequence of the fact that the quasiparticle coherence increases with local hole concentration, as described by Eq. (2). For a low hole concentration we can ignore the last term in Eq. (7b), and obtain

$$H_{kin}=-\sum_{\langle i,j,\sigma\rangle}[t_{ij}+\Delta t_{ij}(\tilde{n}_{i,-\sigma}+\tilde{n}_{j,-\sigma})](\tilde{c}_{i\sigma}^{\dagger}\tilde{c}_{j\sigma}+\text{H.c.}), \quad (8a)$$

$$t_{ij}=S^2t_{ij}^{0}, \quad (8b)$$

$$\Delta t_{ij}=\Upsilon t_{ij}. \quad (8c)$$

Kinetic energy of the form of Eq. (8) is used in the model of hole superconductivity, and leads to pairing and superconductivity for a low hole concentration in the presence of appreciable on-site and nearest-neighbor Coulomb repulsion.[9] The condition for superconductivity to occur is

$$\Upsilon>\sqrt{(1+u)(1+w)}-1, \quad (9)$$

where u and w are dimensionless on-site and nearest-neighbor Coulomb repulsions.[9] Hence, within this class of models, superconductivity is intimately tied to increased quasiparticle coherence. Note that in a model with anisotropy Eq. (8) still implies

$$\frac{\Delta t_{ij}}{t_{ij}}=\Upsilon, \quad (10)$$

independent of direction. This assumption was used in our studies with the model of hole superconductivity,[9] and can be seen to be a necessary consequence of the fact that the Δt term in the Hamiltonian arises from quasiparticle undressing. A necessary consequence of Eq. (10) is that the superconducting energy gap function has the form[9]

$$\Delta_k=\Delta(\epsilon_k), \quad (11)$$

and hence is constant over the Fermi surface ($\epsilon_k=\epsilon_F$), even for an anisotropic band structure. Thus Eq. (11) can be understood as a direct consequence of the undressing physics. Finally, Eq. (8) leads to superconductivity through kinetic-energy lowering.[10] Hence, within the undressing scenario considered here, kinetic-energy lowering as the system becomes superconducting is intimately tied to *s-wave symmetry* of the superconducting order parameter as described by Eq. (11).

III. GREEN'S FUNCTION: COHERENT PART

The single-particle Green's function is given by a sum of coherent and incoherent parts,

$$G_{rs}(\tau)=-\langle Tc_{r\uparrow}(\tau)c_{s\uparrow}^{\dagger}(0)\rangle\equiv G_{rs}^{coh}(\tau)+G_{rs}^{incoh}(\tau), \quad (12)$$

with T the time-ordering operator. The coherent part of the Green's function is obtained by replacing the bare fermion operators in Eq. (12) by its coherent parts, given by Eq. (2) in terms of the quasiparticle operators:

$$G_{rs}^{coh}(\tau)=-S^2\langle T[1+\Upsilon\tilde{n}_{r,\downarrow}(\tau)]\tilde{c}_{r\uparrow}(\tau)\times[1+\Upsilon\tilde{n}_{s,\downarrow}(0)]\tilde{c}_{s\uparrow}^{\dagger}(0)\rangle. \quad (13)$$

The normal and anomalous Green's functions for the quasiparticle operators

$$\tilde{G}_{rs}(\tau)=-\langle T\tilde{c}_{r\uparrow}(\tau)\tilde{c}_{s\uparrow}^{\dagger}(0)\rangle, \quad (14a)$$

$$\tilde{F}_{rs}(\tau) = -\langle T\tilde{c}_{r\uparrow}(\tau)\tilde{c}_{s\downarrow}(0)\rangle \tag{14b}$$

are given in the usual forms[17]

$$\tilde{G}(k,i\omega_n) = \frac{u_k^2}{i\omega_n - E_k} + \frac{v_k^2}{i\omega_n + E_k}, \tag{15a}$$

$$\tilde{F}(k,i\omega_n) = -u_k v_k \left[\frac{1}{i\omega_n - E_k} - \frac{1}{i\omega_n + E_k}\right], \tag{15b}$$

where the coherence factors u_k and v_k and the quasiparticle energies E_k are given by the usual BCS expressions

$$u_k^2 = \frac{1}{2}\left(1 + \frac{\epsilon_k - \mu}{E_k}\right), \tag{16a}$$

$$v_k^2 = \frac{1}{2}\left(1 - \frac{\epsilon_k - \mu}{E_k}\right), \tag{16b}$$

$$u_k v_k = \frac{\Delta_k}{2E_k}, \tag{16c}$$

$$E_k = \sqrt{(\epsilon_k - \mu)^2 + \Delta_k^2}, \tag{16d}$$

and the gap function Δ_k is obtained from the BCS solution of the model of hole superconductivity,[9] i.e., the kinetic energy [Eq. (8)] supplemented with on-site and nearest-neighbor Coulomb repulsion. The single-particle energy ϵ_k in these equations is given by $\epsilon_k = Z(n)\epsilon_k^0 = S^2(1+n\Upsilon)\epsilon_k^0$, with ϵ_k^0 the bare kinetic energy given by the Fourier transform of $(-t_{ij}^0)$.

It can be seen that the extra density operators in Eq. (13) will modify the normal Green's function, introducing anomalous terms similar to the anomalous terms that occur when calculating the expectation value of the kinetic energy [Eq. (7)] that lead to the optical sum rule violation.[10] We expand Eq. (13), keeping only linear terms in the density as appropriate to the low hole concentration regime, and use mean-field decoupling for the averages, to obtain

$$G^{coh}(k,i\omega_n) = S^2[(1+n\Upsilon)\tilde{G}(k,i\omega_n) + 2f_0\Upsilon\tilde{F}(k,i\omega_n)], \tag{17}$$

with $f_0 = \langle \tilde{c}_{i\downarrow}\tilde{c}_{i\uparrow}\rangle$ the on-site pair amplitude in the superconducting state. We also performed a space and time Fourier transform. It can be seen that the normal Green's function has acquired a contribution from the anomalous Green's function due to the density-dependent dressing.

However, the quasiparticle spectral weights derived from Eq. (17) are not positive definite, and in fact can become negative in extreme parameter regimes. To remedy this we need to include higher-order terms obtained from Eq. (13) by keeping terms with six fermion operators. Performing a similar mean-field decoupling for these, we finally obtain for the Green's function,

$$G^{coh}(k,i\omega_n) = \frac{Z_h}{i\omega_n - E_k} + \frac{Z_e}{i\omega_n + E_k}, \tag{18a}$$

with

$$Z_h = S^2[[1+n\Upsilon]u_k - f_0\Upsilon v_k]^2, \tag{18b}$$

$$Z_e = S^2[[1+n\Upsilon]v_k + f_0\Upsilon u_k]^2, \tag{18c}$$

and

$$f_0 = \langle \tilde{c}_{i\downarrow}\tilde{c}_{i\uparrow}\rangle = \frac{1}{N}\sum_k \frac{\Delta_k}{2E_k}[1 - 2f(E_k)]. \tag{18d}$$

The quasiparticle weights Z_h and Z_e are clearly positive definite. Their sum is not conserved as a function of density or temperature because of contributions from the incoherent part of the Green's function not contained in Eq. (13).

In the absence of undressing ($\Upsilon = 0$) the coherent Green's function [Eq. (18)] reduces to the usual BCS form except for the overall factor S^2. In the presence of undressing ($\Upsilon > 0$), Eq. (18) shows that the coherent part of the Green's function and spectral function will increase with hole density n, both for positive and negative energies. Furthermore, as the system becomes superconducting the on-site pair amplitude f_0 develops a positive expectation value. From Eq. (18) this implies that the coherent spectral weight will *decrease* for *positive* energies (hole injection), and *increase* for *negative* energies (hole extraction). The effect on the superconducting state will be largest for parameters where the on-site pair amplitude is large, which corresponds to the short coherence length achieved in the strong-coupling underdoped regime.[15] The magnitude of these effects, both in the normal and superconducting states depends on the magnitude of the undressing parameter Υ. The total quasiparticle weight

$$Z_{tot} = Z_e + Z_h = S^2[(1+n\Upsilon)^2 + \Upsilon^2 f_0{}^2] \tag{18e}$$

will always increase as superconductivity sets in. We discuss the implications of these results in subsequent sections.

IV. RESULTS FOR QUASIPARTICLE WEIGHTS

To illustrate the behavior emerging from the results of Sec. III, we now consider a specific example. The quasiparticle Hamiltonian is given by the kinetic energy [Eq. (8)] supplemented by on-site and nearest-neighbor Coulomb repulsion:

$$H_{Coul} = U\sum_i \tilde{n}_{i\uparrow}\tilde{n}_{i\downarrow} + V\sum_{\langle ij\rangle} \tilde{n}_i\tilde{n}_j. \tag{19}$$

The BCS solution of this Hamiltonian[9] yields the quasiparticle energies

$$E_k = \sqrt{(\epsilon_k - \mu)^2 + \Delta_k^2} = \sqrt{a^2(\epsilon_k - \mu - \nu)^2 + \Delta_0^2}, \tag{20a}$$

$$\Delta_k \equiv \Delta(\epsilon_k) = \Delta_m\left(-\frac{\epsilon_k}{D/2} + c\right), \tag{20b}$$

$$\Delta_0 = \frac{1}{a}\Delta(\mu), \tag{20c}$$

$$\nu = \frac{1}{a}\frac{\Delta_m}{D/2}\Delta_0, \tag{20d}$$

$$a=\frac{1}{\sqrt{1+\left(\frac{\Delta_m}{D/2}\right)^2}}, \tag{20e}$$

with Δ_m and c parameters that depend on temperature and doping. The bandwidth D in these equations is given by

$$D=D_h(1+n\Upsilon), \tag{21}$$

with D_h the bandwidth in the limit of zero hole concentration. The quasiparticle gap, i.e., the minimum quasiparticle excitation energy, is given by

$$E_g=\Delta_0, \tag{22}$$

and occurs at momentum defined by

$$\epsilon_k^{[0]}=\mu+\nu. \tag{23}$$

However, if $\epsilon_k^{[0]}$ is below the bottom of the band, which occurs when the chemical potential is sufficiently below the bottom of the band at low hole concentration, Eq. (22) is not valid, and instead

$$E_g=\sqrt{\left(-\frac{D}{2}-\mu\right)^2+\Delta\left(-\frac{D}{2}\right)}. \tag{24}$$

We consider a two-dimensional square lattice with only nearest-neighbor hopping and $t_{ij}=t_h$ in Eq. (8). The quasiparticle bandwidth as the hole concentration goes to zero is $D_h=2zt_h$, with $z=4$ the number of nearest neighbors to a site. We choose parameters

$$\begin{aligned} D_h&=0.2\ \text{eV},\\ U&=5\ \text{eV},\\ V&=0.65\ \text{eV},\\ \Upsilon&=19.2, \end{aligned} \tag{25}$$

which imply $\Delta t=\Upsilon D_h/2z=0.48$ eV. For the present purposes we need not specify the magnitude of the parameter S^2, which determines the relative weight of coherent and incoherent contributions to the spectral function.

These parameters yield a maximum T_c versus hole concentration of $T_c^{max}=94$ K, as shown in Fig. 1(a), for optimal doping $n\sim 0.045$. The minimum quasiparticle excitation energy at low temperatures is shown in Fig. 1(b). At a low hole concentration it does not go to zero as T_c does, because the chemical potential falls below the bottom of the band and E_g is determined by Eq. (24) rather than by Eq. (22). The behavior of the chemical potential and the bottom of the band versus hole concentration is shown in Fig. 2. The chemical potential crosses the bottom of the band at $n\sim 0.038$, and ϵ_k^0 [Eq. (23)] crosses the bottom of the band at $n\sim 0.034$.

The on-site pair amplitude f_0 that enters in the expressions for the quasiparticle weights is shown in Fig. 3. As a function of doping it approximately follows the behavior of the critical temperature and of the gap parameter Δ_0 (not shown). At low hole doping it goes to zero because the carrier concentration goes to zero, and at high hole doping it goes to zero because the coherence length is diverging.[15] As a function of temperature, f_0 behaves approximately like the gap, going to zero at T_c as $(T_c-T)^{1/2}$.

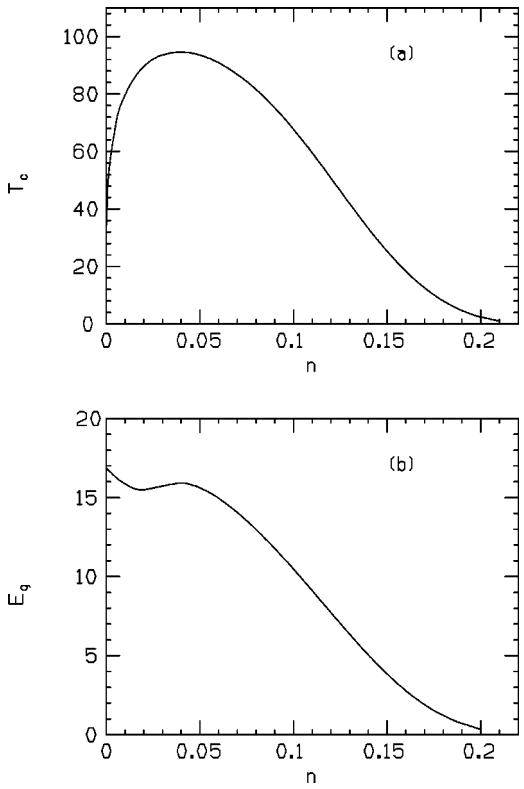

FIG. 1. Superconducting transition temperature vs hole doping n, number of holes per planar oxygen, for parameters given by Eq. (25). (b) Minimum quasiparticle excitation energy at low temperatures vs doping.

Next we consider the behavior of the quasiparticle weights Z_e and Z_h as a function of temperature. Figure 4 shows the results at the (normal state) Fermi energy $\epsilon_k=\mu$ for the optimally doped case ($n=0.045$). The values are normalized so that Z_e and Z_h would be 0.5 for $\Upsilon=0$. The

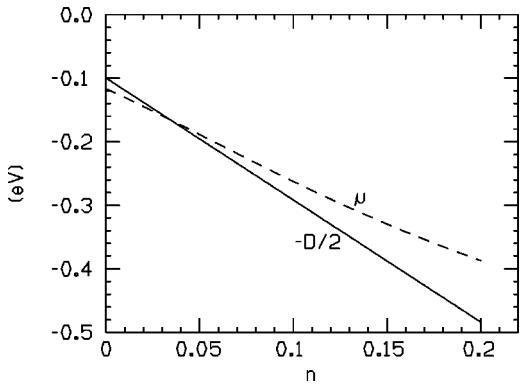

FIG. 2. Chemical potential μ at low temperatures, and band bottom $(-D/2)$ vs hole doping for Eq. (25). The chemical potential falls below the bottom of the band for a hole concentration $n\sim 0.038$. For a fixed hole concentration μ increases as the temperature is lowered above T_c, particularly for a low hole concentration, and stays approximately constant below T_c for all hole concentrations.

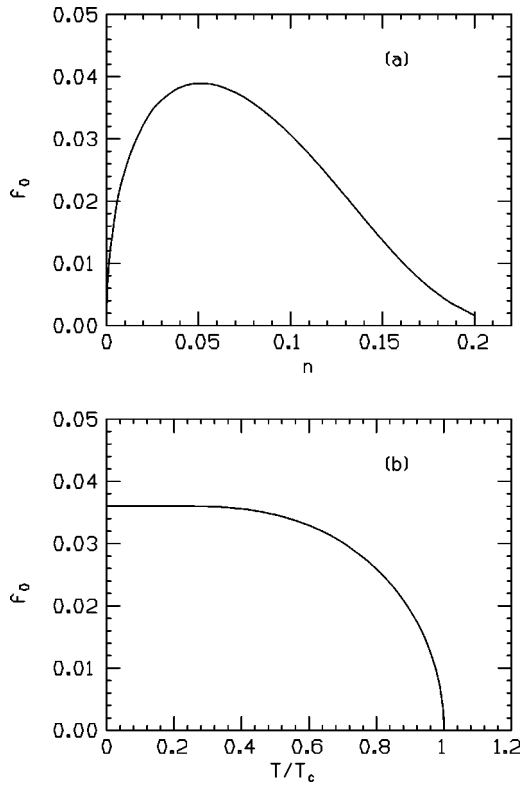

FIG. 3. On-site pair amplitude f_0 (a) vs hole doping at low temperatures, and (b) vs temperature at optimal doping.

dashed line shows the value the weights would have for $f_0=0$: this is temperature independent, and larger than 0.5 because of the undressing due to the average carrier concentration n. The effect of the onset of superconductivity is to increase Z_e as the temperature is lowered, and to decrease Z_h. This indicates that there is extra amplitude for electron creation, and less amplitude for hole creation. This may thus be interpreted as a shift of the chemical potential as superconductivity sets in, causing increased hole occupation as the temperature is lowered, or equivalently a shrinking of the electron Fermi sea. This is a surprising result of this calculation, and its implications will be discussed in subsequent sections. Note that the weight Z_e increases by almost a factor of 2 between $T=T_c$ and $T=0$. The magnitude of the increase of course depends on the magnitude of the undressing parameter Υ, and would be larger or smaller for larger or smaller values of Υ, respectively. By adjusting the values of on-site and nearest-neighbor Coulomb repulsion in the model, it would be possible to obtain the same maximum T_c with different values of Υ, as discussed in previous work.[9] Nevertheless we believe that the parameters chosen for this example may be representative of the situation in high-T_c materials.

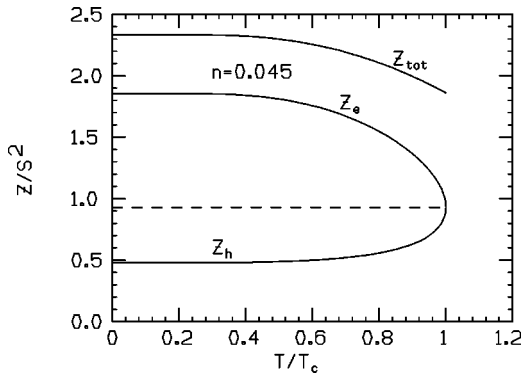

FIG. 4. Quasiparticle weights at the Fermi energy ($\epsilon_k=\mu$) vs temperature for the optimally doped case. $T_c=94$ K. Z_{tot} is the sum of Z_h and Z_e. The corresponding BCS results are equal to each other, and are independent of temperature (dashed line).

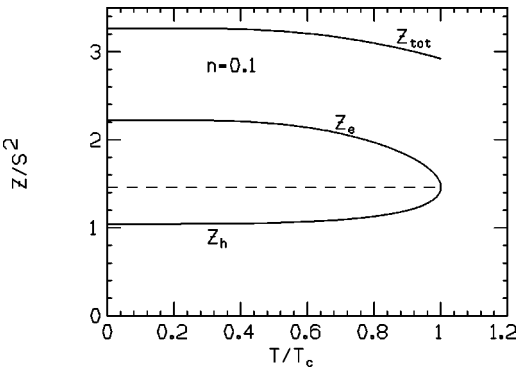

FIG. 5. Same as Fig. 4 for an overdoped case $n=0.1$, with $T_c=68$ K.

Note also that the total weight of the spectral function $Z_{tot}=Z_e+Z_h$ increases as the temperature is lowered below T_c. This indicates that overall there is more coherence in the superconducting state than in the normal state, in accordance with Eq. (18e), and this extra spectral weight is transferred from the high-energy incoherent part of the spectral function as will be discussed in Sec. V. However part of the enhancement of Z_e at low temperatures, relative to its value at T_c can be attributed to spectral weight being transferred from negative to positive energies (i.e., a corresponding depletion of Z_h), in addition to spectral weight transfer from the incoherent part of the spectral function.

Similarly, Fig. 5 shows the results for an overdoped case, $n=0.1$, with $T_c=68$ K. The behavior is qualitatively similar to that in the optimally doped case; however, the effect of the onset of superconductivity on the spectral weights is considerably smaller because the system is already more coherent in the normal state. This is indicated by the larger values of all the spectral weights relative to the values of the case shown in Fig. 4, due to the enhanced coherence arising from the increased hole concentration. For a much higher hole

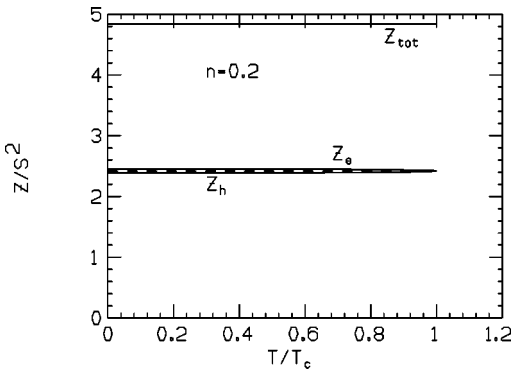

FIG. 6. Same as Fig. 4 for a highly overdoped case $n=0.2$, with $T_c=2.4$ K.

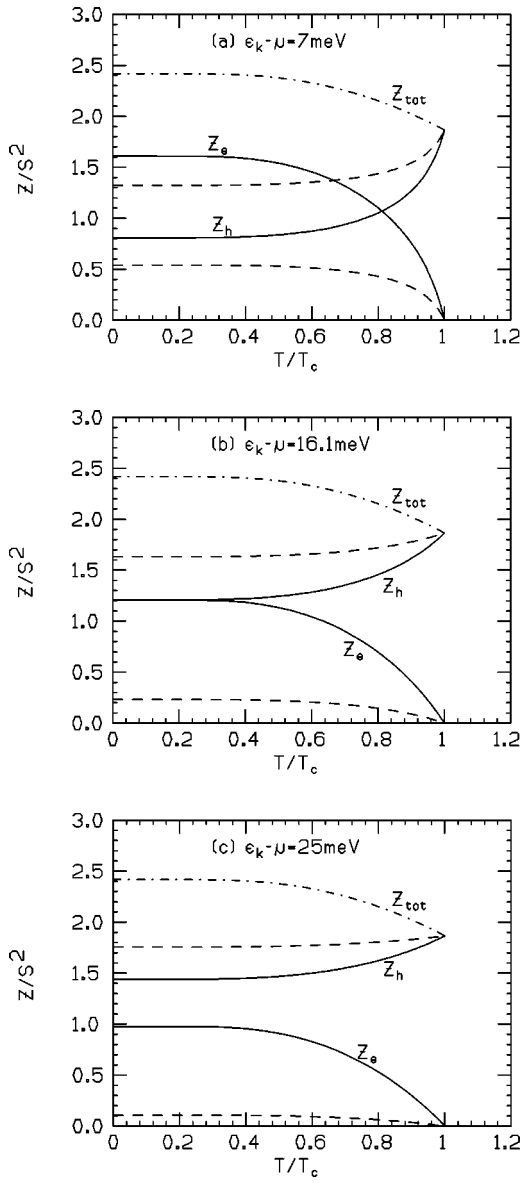

FIG. 7. Spectral weights at optimal doping vs temperature for momentum *inside* the *electron* Fermi surface. The dashed lines give the BCS values [Eq. (18), with $f_0=0$, $u_k^2\sim Z_h$, and $v_k^2\sim Z_h$]. The upper dashed line corresponds to u_k^2, the lower one to v_k^2.

concentration, as T_c approaches zero, the ''gap'' between Z_e and Z_h in the superconducting state closes, as shown in Fig. 6. It always remains nonzero, however, as long as T_c is nonzero, and there is always some spectral weight transfer from the incoherent region as long as T_c is nonzero.

Next we consider the spectral weights for other values of momentum. Figure 7 shows results for $\epsilon_k-\mu>0$. Recall that we are using a hole representation, so $\epsilon_k-\mu>0$ means inside the filled Fermi sea for electrons. In the normal state, $Z_e=0$; since the electron state is full, no new electron can be created in it. Just as in the conventional BCS case, as superconductivity sets in the state becomes partially occupied and $Z_e\neq 0$, and Z_h correspondingly decreases. However, unlike the conventional BCS case, Z_e and Z_h cross in our case, and at low temperatures the weight for creating an electron is larger than that for creating a hole, even though we are inside the filled normal-state Fermi sea. Clearly this implies that the

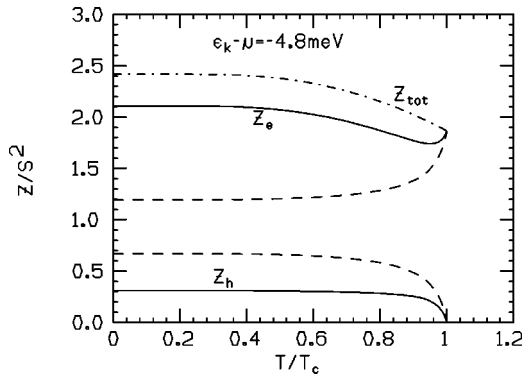

FIG. 8. Spectral weights at optimal doping vs temperature for momentum *outside* the *electron* Fermi surface. The dashed lines give the BCS values. The upper dashed line corresponds to v_k^2, and the lower one to u_k^2.

chemical potential in the superconducting state has changed. Figure 7(b) shows that for $\epsilon_k-\mu=16.1$ meV the weights for electrons and holes coincide at low temperatures; this momentum then corresponds to the new Fermi momentum k_F' in the superconducting state. For even larger ϵ_k, Z_e becomes smaller than Z_h as in the conventional case, as shown in Fig. 7(c).

The behavior for negative energy (outside of the electron Fermi sea) is shown in Fig. 8. Here, $\epsilon_k-\mu$ was chosen to be at the bottom of the hole band in the optimally doped case. The weight for electron creation is much larger than in the conventional case. Note also that Z_e first decreases and then increases as the temperature is lowered, and as $T\rightarrow 0$ it becomes even larger than its value in the normal state. Such a situation, which is never seen in the conventional case, is possible here due to the nonconservation of Z_{tot}, because of the transfer of spectral weight from the incoherent part to the coherent part of the spectral function as the temperature is lowered.

Figure 9 shows the spectral weights for an overdoped case $n=0.1$, for values of the momentum above the electron Fermi surface, at the Fermi surface, and below the Fermi surface. The behavior is qualitatively similar to that for the optimally doped case, although the differences between the conventional case and our case are less pronounced here because this is a weaker coupling regime. In Fig. 10 we show the spectral weight for an underdoped case, $n=0.02$. Here the chemical potential is below the bottom of the band, so a situation comparable to Fig. 4 cannot be attained. Figure 10 shows the behavior of the spectral weight for ϵ_k at its lowest possible value, the bottom of the band, which is qualitatively similar to other cases where ϵ_k is above μ such as Fig. 7(a).

Next we consider the behavior of the quasiparticle weights at the chemical potential versus doping in Fig. 11. The upper dot-dashed line is the total spectral weight in the superconducting state, and the dotted line below it is the total spectral weight in the normal state. The difference between the two is the spectral weight transferred from high-energy incoherent processes as the system becomes superconducting; this difference approaches zero in the overdoped regime. The full lines denote the quasiparticle weights in our case, and the dashed lines the usual BCS results ($u_k^2=Z_h, v_k^2=Z_e$), which increase approximately linearly with n due to

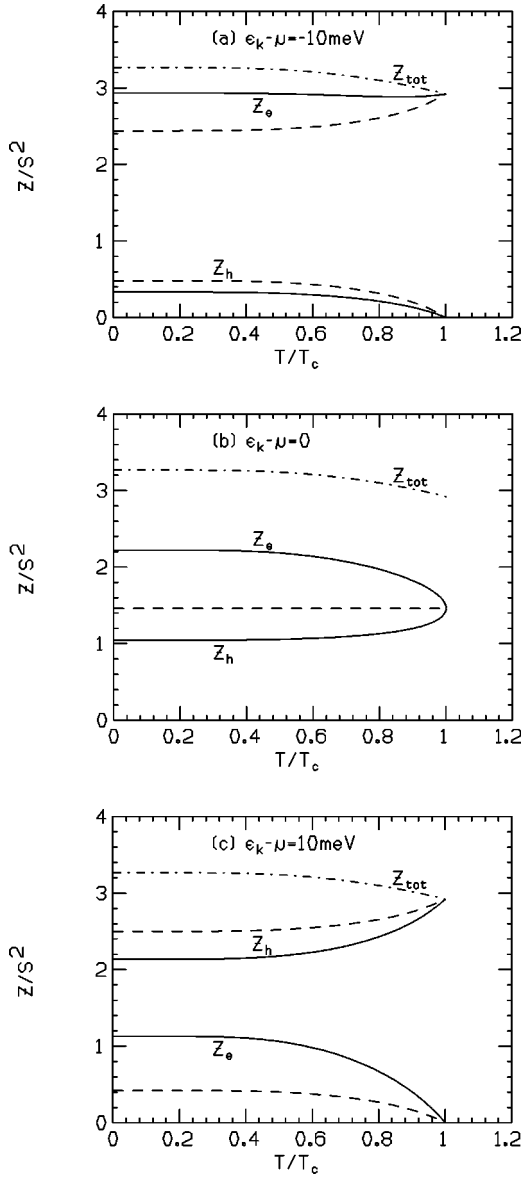

FIG. 9. Spectral weights vs temperature for an overdoped case $n=0.1$, and momentum (a) outside, (b) at, and (c) inside the electron Fermi surface.

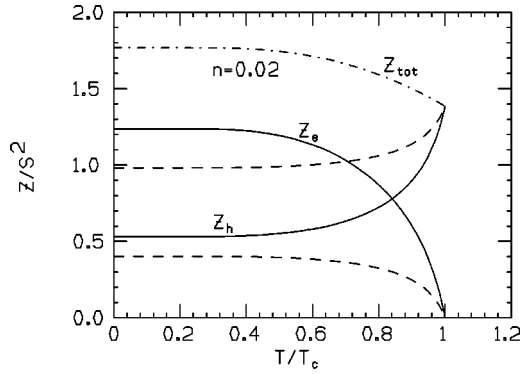

FIG. 10. Spectral weights vs temperature for an underdoped case $n=0.1$, and momentum inside the electron Fermi surface. The value of $\epsilon_k-\mu=6.5$ meV corresponds to ϵ_k at the bottom of the hole band.

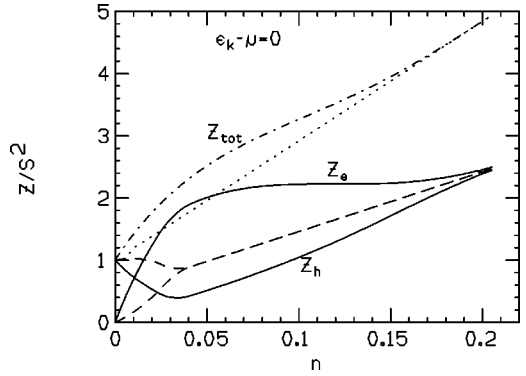

FIG. 11. Quasiparticle weights vs doping at low temperatures. The weights are computed at the chemical potential when it is inside the band, and at the lower hole band edge in the underdoped regime when the chemical potential is below the band edge. The lower dashed line gives the BCS values u_k^2 and v_k^2, which are equal when μ is inside the band, and separate into two (the upper corresponding to u_k^2, and the lower to v_k^2) when μ is below the hole band edge. The dot-dashed line Z_{tot} gives the total weight Z_h+Z_e, and the dotted line close to it the corresponding BCS total weight. Note that Z_e rises approximately linearly with doping for low hole doping, and levels off in the overdoped regime. All results approach the BCS values for high doping as f_0 approaches zero, but remain different from the BCS values as long as T_c is nonzero.

the normal state increased coherence with doping and are equal for $\epsilon_k=\mu$. For low dopings, however, the chemical potential falls below the bottom of the band, and hence we take ϵ_k at the bottom of the band rather than at μ; this is why the two dashed lines diverge at low dopings. In our case, the weight for electron creation (solid curve labeled Z_e) is seen to increase rapidly with doping, and then taper off for high doping; this latter effect is due to the reduction of the on-site pair amplitude f_0 for high doping as the coherence length becomes large.[9] The quasiparticle weights Z_e and Z_h approach each other and the BCS value for high doping, as expected. Note also that there is a narrow doping regime where the electron weight Z_e is even larger than the total weight in the normal state (dotted line). This situation can never occur in the conventional BCS case.

We believe the behavior exhibited by Z_e in Fig. 11 is relevant to the understanding of the angle-resolved photoemission results discussed by Ding *et al.*[1] In their work, the quasiparticle weight in the superconducting state extracted from photoemission spectra shows a qualitative behavior similar to the behavior exhibited by Z_e in Fig. 11. We will discuss the relation between Z_e and the experimental quantity in a subsequent section. Ding *et al.* also plotted $Z\Delta$, the product of their extracted quasiparticle weight and the gap inferred from the photoemission spectra, and pointed out that its behavior roughly follows the bell-shaped curve of T_c. Our calculation shows a similar behavior, as shown in Fig. 12. Note that the quasiparticle gap itself remains finite in our calculation as the hole concentration goes to zero[15] [Fig. 1(b)], and also experimentally.[18]

V. GREEN'S FUNCTION: INCOHERENT PART

To calculate the incoherent part of the Green's function, we now consider a specific model: the generalized Holstein

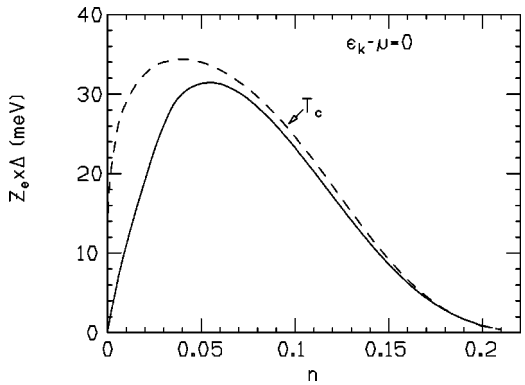

FIG. 12. Product of electron quasiparticle weight Z_e and minimum quasiparticle excitation energy E_g at low temperatures vs hole doping. The dashed line gives T_c vs doping. Note that $Z_e \times \Delta$ peaks at somewhat higher values of hole doping than T_c does.

model discussed in I. Our calculation closely follows the calculation of Alexandrov and Ranninger[19] for the conventional Holstein model, and we refer the reader to their seminal work for details which are common to both situations. The site Hamiltonian for our case is given by[13]

$$H=\hbar\omega_0 a^\dagger a+g\hbar\omega_0(a^\dagger+a)(n_\uparrow+n_\downarrow-\gamma n_\uparrow n_\downarrow)+Un_\uparrow n_\downarrow . \tag{26}$$

The case of Alexandrov and Ranninger corresponds to $\gamma=0$. Using a generalized Lang-Firsov transformation,[13] the quasiparticle (polaron) operators $\tilde{c}_{i\sigma}$ are related to the bare fermion (hole) operators by

$$c_{i\sigma}=\tilde{c}_{i\sigma}X_{i\sigma}, \tag{27a}$$

$$X_{i\sigma}=e^{-g(a_i^\dagger-a_i)(1-\gamma\tilde{n}_{i-\sigma})}. \tag{27b}$$

In contrast to Eq. (2), the operator $c_{i\sigma}$ here is the full hole destruction operator, including coherent and incoherent parts. The coherent part results from the expectation value of the X operators in the zero boson subspace,

$$\langle X_{i\sigma}\rangle=e^{-(g^2/2)(1-\gamma\tilde{n}_{i-\sigma})}, \tag{28}$$

and, in particular,

$$X_{i\sigma}(\tilde{n}_{i-\sigma}=0)=e^{-(g^2/2)}=S, \tag{29a}$$

$$X_{i\sigma}(\tilde{n}_{i-\sigma}=1)=e^{-(g^2/2)(1-\gamma)^2}=T, \tag{29b}$$

in accordance with Eq. (2).

We wish to calculate the Green's function

$$\begin{aligned}G(m,\tau)&=-\langle Tc_{0\uparrow}(\tau)c_{m\uparrow}^\dagger(0)\rangle\\&=-\langle Te^{g[a_0^\dagger(\tau)-a_0(\tau)][1-\gamma\tilde{n}_{0\downarrow}(\tau)]}\tilde{c}_{0\uparrow}(\tau)\\&\quad\times\tilde{c}_{m\uparrow}^\dagger(0)e^{-g[a_m^\dagger(0)-a_m(0)][1-\gamma\tilde{n}_{m\downarrow}(0)]}\rangle.\end{aligned} \tag{30}$$

We expand the exponentials in Eq. (30) using the operator relation

$$e^{g(a^\dagger-a)(1-\gamma\tilde{n}_\downarrow)}=e^{g(a^\dagger-a)}+\tilde{n}_\downarrow(e^{g(a^\dagger-a)(1-\gamma)}-e^{g(a^\dagger-a)}), \tag{31}$$

and decouple averages over bosons and fermions, following Alexandrov and Ranninger. This leads to

$$\begin{aligned}G(m,\tau)&=\sigma_0(m,\tau)\langle -T\tilde{c}_{0\uparrow}(\tau)\tilde{c}_{m\uparrow}^\dagger(0)\rangle+[(\sigma_1(m,\tau)\\&\quad-\sigma_0(m,\tau)][\langle -T\tilde{n}_{0\downarrow}(\tau)\tilde{c}_{0\uparrow}(\tau)\tilde{c}_{m\uparrow}^\dagger(0)\rangle\\&\quad+\langle -T\tilde{c}_{0\uparrow}(\tau)\tilde{c}_{m\uparrow}^\dagger(0)\tilde{n}_{m\downarrow}(0)\rangle]+[\sigma_2(m,\tau)\\&\quad-2\sigma_1(m,\tau)+\sigma_0(m,\tau)]\\&\quad\times\langle -T\tilde{n}_{0\downarrow}(\tau)\tilde{c}_{0\uparrow}(\tau)\tilde{c}_{m\uparrow}^\dagger(0)\tilde{n}_{m\downarrow}(0)\rangle.\end{aligned} \tag{32}$$

The boson Green's functions are defined as

$$\sigma_{i+j}(m,\tau)=\langle e^{g(1-\gamma)^i[a_0^\dagger(\tau)-a_0(\tau)]}e^{-g(1-\gamma)^j[a_m^\dagger(0)-a_m(0)]}\rangle, \tag{33}$$

with $i,j=0,1$. At low temperatures they are given by[20]

$$\sigma_\alpha(m,\tau)=S^{2-\alpha}T^\alpha[1-\delta_{m,0}+\delta_{m,0}e^{-g^2(1-\gamma)^\alpha D(\tau)}], \tag{34a}$$

$$D(\tau)=-\left[e^{-\omega_0|\tau|}+2\frac{\cosh\omega_0\tau}{e^{\beta\omega_0}-1}\right], \tag{34b}$$

and in frequency space by

$$\sigma_\alpha(m,i\omega_n)=S^{2-\alpha}T^\alpha\left[\delta_{n,0}\beta+\delta_{m,0}\sum_{l=1}^{\infty}\frac{2l\omega_0 g^{2l}(1-\gamma)^{\alpha l}}{l!(\omega_n^2+l^2\omega_0^2)}\right]. \tag{35}$$

We next decouple the fermion averages with the same mean-field procedure used to calculate the coherent part of the Green's function, and calculate the Fourier transform

$$G(k,i\omega_n)=\int_0^\beta d\tau e^{i\omega_n\tau}\sum_m e^{ikm}G_{0m}(\tau). \tag{36}$$

The complete Green's function is

$$G(k,i\omega_n)=G_{coh}(k,i\omega_n)+G_{inc}(k,i\omega_n). \tag{37}$$

For each term of the coherent Green's function [Eq. (18)], there is a corresponding term in the incoherent Green's function. All terms in the coherent Green's function are of the form

$$G_{coh}^{\alpha,s}(k,i\omega_n)=cS^{2-\alpha}T^\alpha\frac{a_k}{i\omega_n-sE_k}, \tag{38}$$

with $0\leqslant\alpha\leqslant2$ and $s=+/-1$. The corresponding term in the incoherent Green's function is

$$\begin{aligned}G_{inc}^{\alpha,s}(k,i\omega_n)&=cS^{2-\alpha}T^\alpha\sum_{l=1}^{\infty}\frac{g^{2l}(1-\gamma)^{\alpha l}}{l!}\frac{1}{N}\\&\quad\times\sum_{k'}a_{k'}\left[\frac{n_{k'}}{i\omega_n-s(E_{k'}-l\omega_0)}\right.\\&\quad\left.+\frac{1-n_{k'}}{i\omega_n-s(E_{k'}+l\omega_0)}\right].\end{aligned} \tag{39}$$

The spectral function is obtained as usual from

$$A(k,\omega) = -\,\mathrm{Im}\, G(k, i\omega_n \rightarrow \omega + i\delta), \tag{40}$$

and results from Eqs. (18) and (37)–(39). In particular, the lowest-order normal part of the incoherent spectral function is given by

$$A^n_{inc}(k,\omega) = S^2 \times \sum_{l=1}^{\infty} \frac{g^{2l}}{l!}\{1 + n[(1-\gamma)^l e^{\gamma g^2} - 1]\}\frac{1}{N} \times \sum_{k'} \{u^2_{k'}[(1-n_{k'})\delta(\omega - l\omega_0 - E_{k'}) + n_{k'}\delta(\omega + l\omega_0 - E_{k'})] + v^2_{k'}[n_{k'}\delta(\omega - l\omega_0 + E_{k'}) + (1-n_{k'})\delta(\omega + l\omega_0 + E_{k'})]\}, \tag{41}$$

and the lowest-order anomalous contribution by

$$A^a_{inc}(k,\omega) = S^2 \times 2f_0 \times \sum_{l=1}^{\infty} \frac{g^{2l}}{l!}\{1 + n[(1-\gamma)^l e^{\gamma g^2} - 1]\}\frac{1}{N} \times \sum_{k'} (-u_{k'}v_{k'}) \times [(1-n_{k'})\delta(\omega - l\omega_0 - E_{k'}) + n_{k'}\delta(\omega + l\omega_0 - E_{k'}) - n_{k'}\delta(\omega - l\omega_0 + E_{k'}) - (1-n_{k'})\delta(\omega + l\omega_0 + E_{k'})]. \tag{42}$$

VI. RESULTS FOR THE SPECTRAL FUNCTION

The spectral functions for the models considered here are of the forms

$$A(k,\omega) = A_{coh}(k,\omega) + A_{inc}(k,\omega), \tag{43a}$$

$$A_{coh}(k,\omega) = Z_h\delta(\omega - E_k) + Z_e\delta(\omega + E_k), \tag{43b}$$

$$A_{inc}(k,\omega) = -\,\mathrm{Im}\, G_{inc}(k, \omega + i\delta), \tag{43c}$$

where the quasiparticle weights Z_h and Z_e, and the incoherent Green's function G_{inc}, were discussed in Secs. IV and V. As seen in Sec. IV, the quasiparticle weight Z_e acquires a *positive* contribution from the onset of superconductivity. In a spectroscopic experiment, usually only one side of the spectral function is sampled, as the other side is suppressed by the Fermi function. The quantity that will display the enhanced coherence, due to undressing exhibited by Z_e, is

$$I_0(k,\omega) = A(k,\omega)f(\omega), \tag{44}$$

with f the Fermi function. In an experiment there will typically be broadening from experimental resolution, which results in

$$I(k,\omega) = \int d\omega' F(\omega - \omega') I_0(k,\omega') \tag{45}$$

being measured, with $F(\omega)$ a Gaussian with width σ_ω. There could also be other sources of broadening of the δ functions in the expressions [Eqs. (43)] from lifetime effects. Just like the spectral function, the measured spectrum [Eq. (45)] will have coherent and incoherent contributions

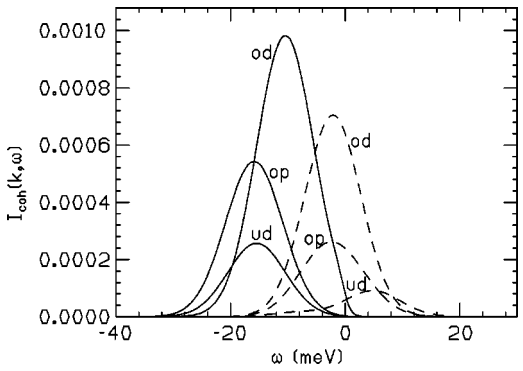

FIG. 13. Coherent part of the spectral function multiplied by the hole Fermi function $f(\omega)$ and broadened by a Gaussian function [Eq. (43)], with $\sigma_\omega = 5$ meV. The dashed lines give the results at T_c, the full lines the results at low temperatures ($T = 0.1T_c$). od, op, and ud denote overdoped ($n = 0.1$), optimally doped ($n = 0.045$) and underdoped ($n = 0.02$) regimes.

$$I(k,\omega) = I_{coh}(k,\omega) + I_{inc}(k,\omega), \tag{46}$$

arising from the coherent and incoherent parts of the spectral function, respectively.

Figure 13 shows results for the coherent spectra at the Fermi energy for an underdoped ($n = 0.02$, labeled ud), optimally doped ($n = 0.045$, labeled op), and overdoped ($n = 0.1$, labeled od) case for the parameter values used in Sec. V. For the underdoped case with a chemical potential below the bottom of the band, the value of ϵ_k at the bottom of the band was used. The dashed lines show the spectra in the normal state at T_c, and the full lines in the superconducting state at $T = 0.1T_c$. For each doping, as superconductivity onsets, the peaks shift to the left due to the opening of the superconducting gap. Furthermore, the peaks *grow* in magnitude due to the behavior of Z_e discussed in Sec. IV. As a function of doping the peaks grow in magnitude both in the normal and superconducting states, due to the enhanced coherence with an increasing number of carriers. The superconducting peak in the od case is shifted to the right with respect to the op case, because the superconducting gap is smaller in that region [Fig. 1(b)].

When we include the incoherent part of the spectra, the smaller normal-state peak can become almost invisible. The results will of course depend on the specific parameters chosen to describe the incoherent background, and we are not suggesting that we are in a position to determine them from first principles. In Fig. 14, we show results for a particular set of parameters for the generalized Holstein model. In addition to the parameters already discussed in Sec. IV, including the value of Υ, the new parameters needed are S^2, ω_0, and a broadening factor given in the figure caption. Note that in the underdoped case (a) the peak in the normal state has become almost invisible, while a sharp peak and a dip are seen in the superconducting spectrum. The dip arises because the background term arising from the second term in Eq. (39) for $a_{k'} = v^2_{k'}$, $s = -1$, is pushed to more negative energies as the superconducting gap opens. As the doping increases the normal-state peak becomes more visible, and the overdoped case shows more conventional behavior. Note that the scale in the figures changes with doping, and the magnitude of the peaks increases with doping.

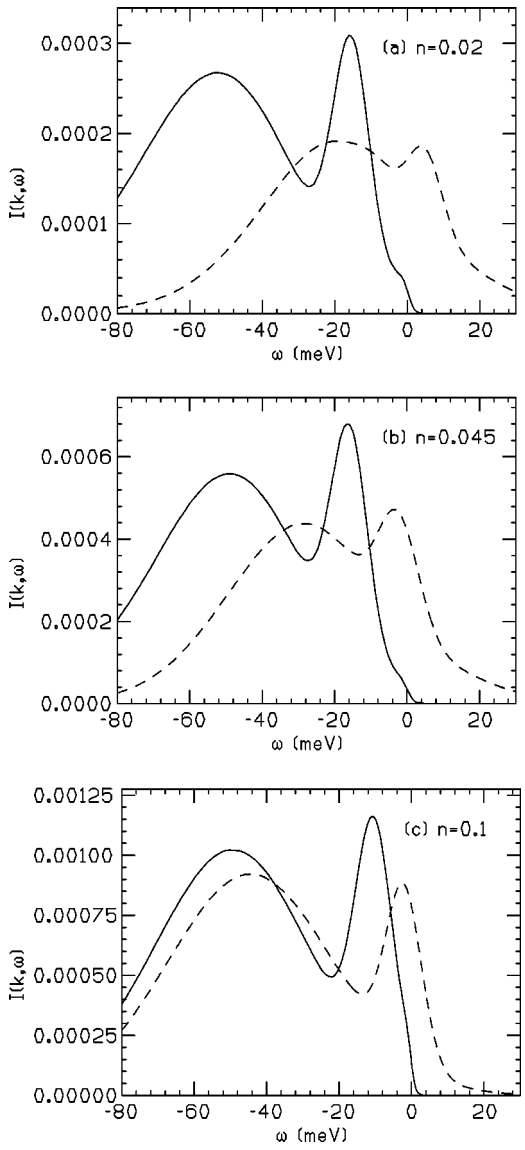

FIG. 14. Results for the full spectra [Eq. (43)] at $T=T_c$ (dashed lines) and at low temperatures, $T=0.1T_c$ (solid lines). The incoherent part of the spectrum was modeled with a generalized Holstein model with $\omega_0=5$ meV and Gaussian broadening for the δ functions $\sigma=15$ meV. The band narrowing parameter is $S^2=1/500$, and $\Upsilon=19.2$, corresponding to $g=2.49$ and $\gamma=0.45$ in Eq. (26). The momentum is given by the normal-state Fermi momentum for the optimally doped and overdoped cases, and by the momentum corresponding to the bottom of the hole band for the underdoped case.

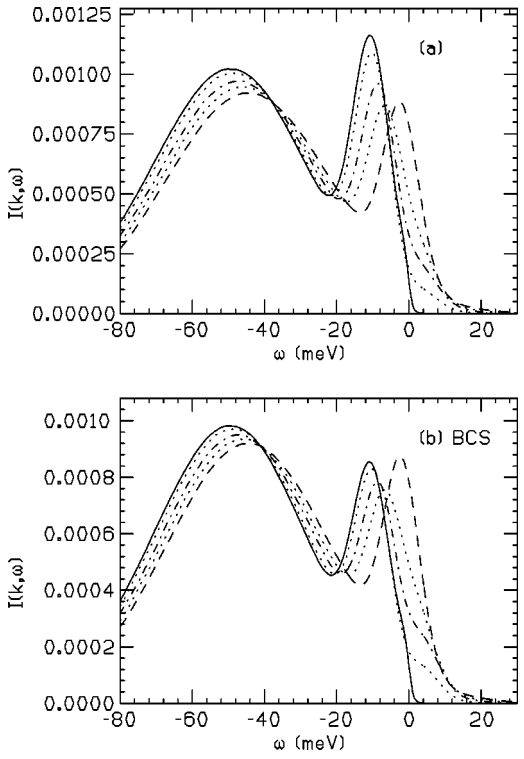

FIG. 15. Spectra in the overdoped case $n=0.1$ at the chemical potential for various temperatures. The dashed, dotted, dot-dashed, dotted, and full lines, with the peak moving toward the left, correspond to $T/T_c=1$, 0.9, 0.8, 0.6, and 0.1 respectively. In (b) the corresponding results for the BCS case, taking $f_0=0$ in Eq. (18), are shown. Note that the peaks in the superconducting state are always lower than that in the normal state in the BCS case.

Figure 15 shows the temperature dependence of the spectra for the overdoped case. The normal-state peak is pushed back continuously as the superconducting gap opens up. In addition, for our case (a) the peak grows in magnitude. To highlight the difference with conventional BCS theory, in Fig. 15(b) we show what is obtained with the same parameters in the absence of the term f_0 in Eq. (18). The peak here first becomes lower, and then increases again as the temperature is lowered, but it is always lower than or equal to the normal state peak. It is easily seen from the BCS formula that this property is generally also true for other values of the momenta.

Similarly, Fig. 16 shows the temperature dependence of the spectra in the underdoped case. Here, rather than the peak moving continuously, a new peak grows in the superconducting state. The presence of two peaks has not been seen experimentally in photoemission, to our knowledge, possibly because of experimental resolution. For the BCS case (b) the peak in the superconducting state is much smaller than in the normal state, while for our case (a) the opposite is true. Results for the temperature dependence in the optimally doped case show a behavior intermediate between the overdoped and underdoped cases shown.

VII. CUPRATES

We saw in previous sections that in systems where superconductivity arises from undressing, there is a signature of the formation of the condensate in the single-particle spectral function. Specifically, it arises in Eq. (17) from the term involving f_0, the on-site pair amplitude. Ding *et al.*[1] and Feng *et al.*,[2] discussing experimental results of angle-resolved photoemission in cuprates, recently emphasized precisely that feature of the observed spectra, and correlated the growth of the peak in photoemission to quantities related to the superconducting condensate such as the superfluid density and the condensation energy. The spectra calculated within the present theory in Sec. VI resemble in several aspects the experimental observations in photoemission along the $(\pi,0)$ direction.

Unfortunately, as the alert reader has undoubtedly noticed, the results presented in Sec. VI, with negative ω in a

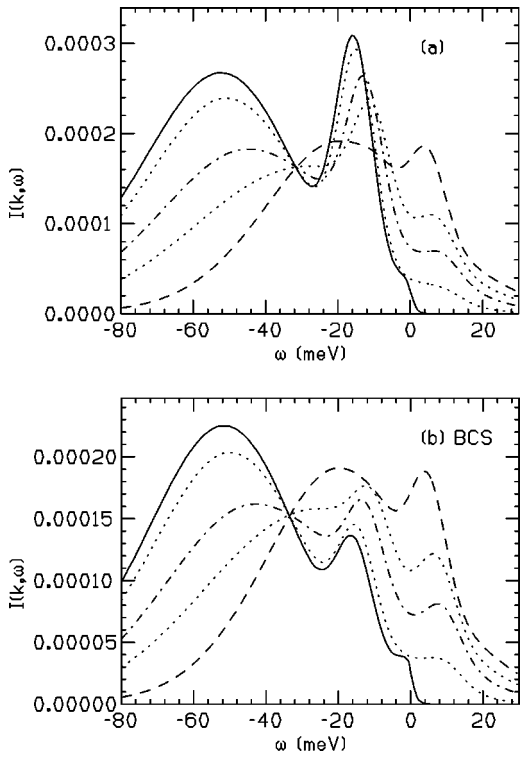

FIG. 16. Same as Fig. 15 for an underdoped case $n=0.02$, for a momentum corresponding to the bottom of the hole band. The same line convention as in Fig. 15 is used.

hole representation, correspond to *hole destruction*, or *electron creation*, that is, *inverse photoemission*. It is for this case that the experiment would sample Z_e, the quasiparticle weight for electron creation. Instead, if we calculate spectra for direct photoemission, we would find that quasiparticle peaks are *suppressed* by the onset of superconductivity due to the behavior of Z_h discussed in Sec. IV.

The present theory does not allow for a switch in the role of the weights Z_e and Z_h: electron-hole asymmetry, of the sign assumed here, is central to the theory. Does this then imply that the theory is irrelevant for description of the cuprates?

We believe this is not the case. We propose that, in fact, the photoemission experiments along the $(\pi,0)$ direction close to the $(\pi/a,0)$ point sample the part of the spectral function discussed in Sec. VI, corresponding to hole destruction or electron creation.

How can photoemission sample electron creation? Recall that in the theory of hole superconductivity the relevant orbitals are oxygen $p\pi$ orbitals in the planes.[8] There are, however, also oxygen $p\sigma$ orbitals, strongly hybridized with the Cu $d_{x^2-y^2}$ orbitals. Suppose that in a photoemission experiment along the $(\pi,0)$ direction the largest matrix element couples to the destruction of a $d_{x^2-y^2}$ electron. This would not directly couple to the band responsible for superconductivity; however, that process could induce the destruction of an oxygen hole in the $p\pi$ orbitals. The proposed situation is schematically depicted in Fig. 17, in an electron representation. Before the photon comes in there is one electron in each Cu^{2+} atom neighbor to a given O atom, and two holes in the $p\pi$ orbital on that O atom. We assume the energy-level structure shown in Fig. 17: an electron from Cu^{2+} cannot

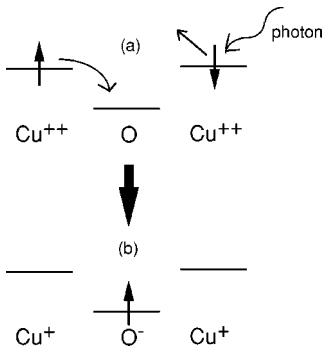

FIG. 17. Schematic proposed explanation of how electron extraction in a photoemission experiment can give rise to hole destruction in the oxygen band responsible for superconductivity. The Cu energy level arises from a hybridized Cu $d_{x^2-y^2}$-O $p\sigma$ orbital, the O energy level corresponds to an O $p\pi$ planar orbital. In (a), an electron in the Cu $d_{x^2-y^2}$ orbital is knocked out by an incoming photon; the electron from a neighboring $d_{x^2-y^2}$ orbital, then falls onto the O $p\pi$ orbital (b), destroying an O hole.

''fall'' onto the O $p\pi$ orbital because it is Coulomb repelled by the electron in the other Cu atom. When a photon comes in and knocks out one of the electrons in a Cu, the other electron can fall onto the O $p\pi$ orbital, thus destroying an O hole and sampling the quasiparticle weight Z_e.

It is clear that this qualitative explanation needs further elaboration and experimental confirmation to be convincing. Nevertheless we also point out that it suggests an explanation for why the sharp peaks seen in photoemission along the $(\pi,0)$ direction are not seen along the (π,π) direction:[21] since Cu $d_{x^2-y^2}$ orbitals point along the principal axis in the planar square lattice, the coupling to the photon along the (π,π) direction is likely to be much smaller. For that direction the larger coupling may be to the O $p\pi$ band itself, in which case inverse rather than direct photoemission would show the enhanced coherence. It is possible that some indication of this effect may have already been seen in tunneling experiments.[22]

VIII. CONCLUSIONS

In this paper we have continued to explore the consequences of the physical principle proposed in I: that, in at least some electronic materials in nature, the dressing of quasiparticle carriers is a function of the local carrier concentration, and becomes smaller as the local carrier concentration increases. This physical principle leads to superconductivity occurring in these systems because of a lowering of the carrier's kinetic energy upon pairing. The superconducting transition, and many of the features of the superconducting state, were already discussed within the theory of hole superconductivity.[8,9,15]

In this paper we explored the consequences of this principle for the single-particle Green's function in the superconducting state. The central result of this paper [Eq. (18)], demonstrates that formation of the superfluid condensate will influence the behavior of the single-particle spectral function. Equation (18) is thus a generalization of the BCS spectral function for systems where superconductivity is driven by undressing. Surprisingly, the results show that the en-

hanced coherence in the superconducting state is displayed in the quasiparticle weight for electron creation but not for electron destruction. We calculated the behavior of the quasiparticle weights as a function of temperature, doping dependence, and momentum, and highlighted the differences from conventional BCS theory.

Furthermore, we discussed the calculation of the full spectral function, including the incoherent contribution, for one particular model where superconductivity occurs through undressing, a generalized Holstein model. Our calculation was performed within the Lang-Firsov approximation,[19] and it should be interesting to see whether the qualitative results survive a more exact treatment.[23,24]

Results for the full spectral function showed several features that resemble experimental observations in photoemission experiments in high-T_c cuprates,[1,2] in particular enhanced coherence, as displayed by the quasiparticle peak in the spectra, when the system enters the superconducting state and as the carrier concentration increases both in the normal and superconducting states.

This study was strongly motivated by the experimental results and insightful analysis of previous photoemission experiments.[1,2] Thus it is perhaps disappointing that at the end of the day our calculation predicted these effects, in the simplest one-band model, to arise in *inverse* rather than in direct photoemission. Thus some readers may conclude that our calculation is not more than an academic exercise. However, as discussed in Sec. VII, we believe there is a plausible scenario by which the spectral weight for electron creation would be sampled in the photoemission experiments in the cuprates.

While the theory discussed here predicts *s*- rather than *d*-wave superconductivity, we believe it is remarkable how many of the features that appear to be part of the phenomenology of high-T_c cuprates it exhibits, as a consequence of the *single assumption* of a large value of the undressing parameter Υ: (1) incoherence in the normal state at low hole concentration; (2) increased coherence with doping in the normal state; (3) transition to superconductivity for low doping, its disappearance for high doping, and bell-shaped T_c versus hole concentration; (4) increased coherence as the system goes superconducting; (5) a superconducting transition driven by kinetic energy lowering, optical sum rule violation; and (6) a nondecrease of the quasiparticle gap at low hole density when T_c goes to zero. This latter feature arises in our model from the fact that as the hole concentration decreases and the band becomes narrower, the chemical potential falls below the bottom of the band;[15] we believe that many of the unusual properties of underdoped cuprates follow from this simple fact, and in particular that the observed pseudogap is simply the energy difference between the bottom of the band and the chemical potential.[25,26]

If the theory of hole undressing discussed here describes the cuprates, it is likely that it is more generally applicable because it is based on very general principles. In this regard we note that one of the paradoxes of the conventional explanation of superconductivity is that it is thought to originate in an electron-boson (the electron phonon) coupling that *opposes conductivity*, i.e., gives rise to resistivity, in the normal state. In a sense the present theory eliminates this paradox. Coupling to a boson is certainly necessary, and that coupling gives rise to enhanced resistivity in the normal state due to enhanced effective mass, but superconductivity arises from a process whereby the coupling to that boson is *reduced* as carriers pair and the system becomes superconducting. However, the old paradox is replaced by a new one: that in order for heavily dressed ''confined'' carriers to become less dressed, or ''freer,'' it is necessary for them to *bind* in Cooper pairs.

We also note that the principle on which the present theory is based, that an increase in the local hole occupation causes undressing, is likely to be more general than as expressed by Eq. (2): rather than just be enhanced by the same site occupation, undressing may also be enhanced by hole occupation of neighboring sites, and also by neighboring bond occupation. Possible implications of this for superconductivity and other instabilities of metals will be discussed in future work.

If indeed the essential physics of high-T_c cuprates is hole undressing, what makes a material a high-T_c superconductor? Presumably, the fact that quasiparticles are heavily dressed in the normal state, together with the fact that the undressing process that occurs when the local carrier concentration increases is particularly efficient. Both these facts are necessary conditions for high-T_c superconductivity, by giving rise to a large Υ parameter. Here we will not discuss what aspects of the chemistry of the cuprates would favor this situation.[27] However, conversely, we may conclude that the reason for a material *not* being a high-T_c superconductor would be a small value of the parameter Υ, either because quasiparticles are *not* heavily dressed in the normal state (e.g., the case of aluminum), or, because the quasiparticle dressing in the normal state may not be strongly dependent on the local carrier concentration (e.g., the case of ''heavy fermion'' systems).

ACKNOWLEDGMENTS

The author is grateful to F. Driscoll for the donation of a computer where the calculations reported here were performed.

[1] H. Ding, J. R. Engelbrecht, Z. Wang, J. C. Campuzano, S.-C. Wang, H.-B. Yang, R. Rogan, T. Takahashi, K. Kadowaki, and D. G. Hinks, cond-mat/0006143 (unpublished), and references therein.

[2] D. L. Feng, D. H. Lu, K. M. Shen, C. Kim, H. Eisaki, A. Damascelli, R. Yoshizaki, J.-I. Shimoyama, K. Kishio, G. D. Gu, S. Oh, A. Andrus, J. O'Donnell, J. N. Eckstein, and Z.-X. Shen, Science **289**, 277 (2000), and references therein.

[3] A. V. Puchkov, T. Timusk, M. A. Karlow, S. L. Cooper, P. D. Han, and D. A. Payne, Phys. Rev. B **54**, 6686 (1996).

[4] D. N. Basov, S. I. Woods, A. S. Katz, E. J. Singley, R. C. Dynes, M. Xu, D. G. Hinks, C. C. Homes, and M. Strongin, Science **283**, 49 (1999); A. S. Katz, S. I. Woods, E. J. Singley, T. W. Li, M. Xu, D. G. Hinks, R. C. Dynes, and D. N. Basov, Phys. Rev.

B **61**, 5930 (2000).
[5] D. van der Marel, A. Tsvetkov, M. Grueninger, D. Dulic, and H. J. A. Molegraaf, Physica C **341–348**, 1531 (2000); *Proceedings of the 10th Annual HTS Workshop on Physics, Houston* (World Scientific, Singapore, 1996), p. 357; J. Schutzmann, H. S. Somal, A. A. Tsvetkov, D. van der Marel, G. E. J. Koops, N. Koleshnikov, Z. F. Ren, J. H. Wang, E. Brück, and A. A. Menovsky, Phys. Rev. B **55**, 11 118 (1997); K. A. Moler, J. R. Kirtley, D. G. Hinks, T. W. Li, and Ming Xu, Science **279**, 1193 (1998); P. W. Anderson, Physica C **341–348**, 9 (2000).
[6] J. C. Campuzano, H. Ding, M. R. Norman, H. M. Fretwell, M. Randeria, A. Kaminski, J. Mesot, T. Takeuchi, T. Sato, T. Yokoya, T. Takahashi, T. Mochiku, K. Kadowaki, P. Guptasarma, D. G. Hinks, Z. Konstantinovic, Z. Z. Li, and H. Raffy, Phys. Rev. Lett. **83**, 3709 (1999); M. R. Norman, H. Ding, J. C. Campuzano, T. Takeuchi, M. Randeria, T. Yokoya, T. Takahashi, T. Mochiku, and K. Kadowaki, *ibid.* **79**, 3506 (1997).
[7] M. R. Norman, M. Randeria, B. Janko, and J. C. Campuzano, Phys. Rev. B **61**, 14 742 (2000).
[8] J. E. Hirsch and S. Tang, Solid State Commun. **69**, 987 (1989); Phys. Rev. B **40**, 2179 (1989); J. E. Hirsch and F. Marsiglio, *ibid.* **41**, 2049 (1990).
[9] J. E. Hirsch and F. Marsiglio, Phys. Rev. B **39**, 11 515 (1989); **45**, 4807 (1992); Physica C **162-164**, 591 (1989); F. Marsiglio and J. E. Hirsch, Phys. Rev. B **41**, 6435 (1990).
[10] J. E. Hirsch, Physica C **199**, 305 (1992); J. E. Hirsch and F. Marsiglio, *ibid.* **331**, 150 (2000); cond-mat/0004496, Phys. Rev. B (to be published 1 December 2000).
[11] J. E. Hirsch, Physica C **201**, 347 (1992); and in *Polarons and Bipolarons in High-T_c Superconductors and Related Materials*, edited by E. K. H. Salje, A. S. Alexandrov, and W. Y. Liang (Cambridge University Press, Cambridge, 1995), p. 234.
[12] I. Fugol, V. Samovarov, A. Ratner, V. Zhuravlev, G. Saemann-Ischenko, B. Holzapfel, and O. Meyer, Solid State Commun. **86**, 385 (1993).
[13] J. E. Hirsch, preceding paper, Phys. Rev. B **62**, 14 487 (2000).
[14] P. Nozieres, *Theory of Interacting Fermi Systems* (Benjamin, New York, 1964), Chap. 4.
[15] F. Marsiglio and J. E. Hirsch, Physica C **165**, 71 (1990); J. E. Hirsch, *ibid.* **161**, 185 (1989).
[16] J. E. Hirsch, Physica C **179**, 317 (1991).
[17] J. R. Schrieffer, *Theory of Superconductivity* (Addison-Wesley, Redwood City, CA, 1988).
[18] N. Miyakawa, J. F. Zasadzinski, L. Ozyuzer, P. Guptasarma, D. G. Hinks, C. Kendziora, and K. E. Gray, Phys. Rev. Lett. **83**, 1018 (1999).
[19] A. S. Alexandrov and J. Ranninger, Physica C **198**, 360 (1992).
[20] G. D. Mahan, *Many-Particle Physics* (Plenum, New York, 1981).
[21] T. Valla, A. V. Fedorov, P. D. Johnson, B. O. Wells, S. L. Hulbert, Q. Li, G. D. Gu, and N. Koshizuka, Science **285**, 2110 (1999).
[22] S. H. Pan, E. W. Hudson, K. M. Lang, H. Eisaki, S. Uchida, and J. C. Davis, Nature (London) **403**, 746 (2000).
[23] F. Marsiglio, Phys. Lett. A **180**, 280 (1993).
[24] C. Zhang, E. Jeckelmann, and S. R. White, Phys. Rev. B **60**, 14 092 (1999).
[25] J. E. Hirsch and F. Marsiglio, Physica C **195**, 355 (1992).
[26] F. Marsiglio and J. E. Hirsch, Phys. Rev. B **44**, 11 960 (1991).
[27] J. E. Hirsch, Chem. Phys. Lett. **171**, 161 (1990); Phys. Rev. B **48**, 3340 (1993).